Nanoscale

Accepted Manuscript

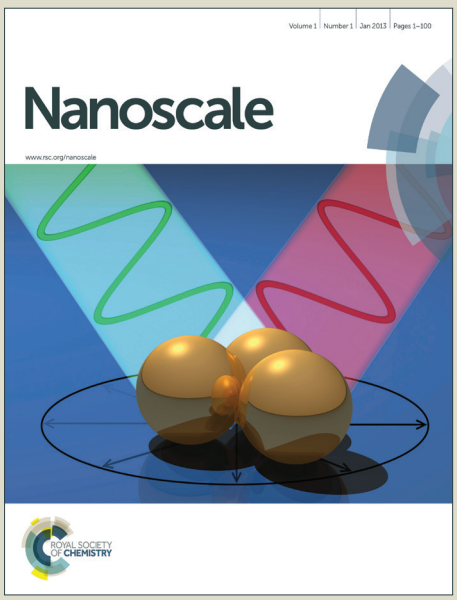

ROYAL SOCIETY OF CHEMISTRY

www.rsc.org/nanoscale

Journal Name

COMMUNICATION

Plasmon enhanced visible light photocatalysis for TiO_2 supported Pd nanoparticles

Received 00th January 20xx,
Accepted 00th January 20xx

DOI: 10.1039/x0xx00000x

www.rsc.org/

A. M. Lacerda,[a] I. Larrosa*[b] and S. Dunn*[a]

A photocatalyst consisting of nanostructured Pd photochemically deposited on 20nm TiO_2 displays a reaction half-life for rhodamine b decolourisation of 0.5 minutes compared to the 9.4 minutes for unmodified P25 under identical reaction conditions. We associate this increase decolourisation rate to the increase in solar light harvesting which we have measured at 8% due to a significant red shift in the absorption profile of the catalyst. We associate the increased absorption of light with a visible active plasmon effect that is associated with the Pd nanostructures on the TiO_2. This overall red-shift in the light harvesting for the catalyst leads to photocatalytic activity for excitations up to 600 nm.

The use of commercial dyes by manufacturing industries such as the textile, pharmaceutical, paint and cosmetic industries regularly results in the release of excess contaminants into the local environment posing a threat to both aquatic and human populations.[1] A promising method for the effective treatment of this industrial effluent is via photocatalysis. Of the photocatalytic materials used in the remediation of environmental pollution, titanium dioxide (TiO_2) has been one of the most studied catalysts.[2–6] Due to its low toxicity, high chemical stability and photosensitivity, TiO_2 is a promising material in a wide range of applications from environmental depollution to the production of solar fuels.[7–13] However, its energy band gap value of 3.2 eV limits the photo-functionality of TiO_2 to the UV region of the electromagnetic (EM) spectrum. As only around 4% of solar irradiation incident on the surface of the Earth is in the UV, many efforts have been made to increase the absorption cross-section of TiO_2 photocatalysts into the visible region.[14–16] Recently there has been interest in investigating 'functional materials' for increasing light harvesting efficiency with large band gap semiconductors, but there still remains a significant effort to increase the absorption spectrum for materials such as TiO_2. [17,18]

A well-studied approach to increasing the light harvesting ability for TiO_2 has been to decorate the surface of the catalyst with nanostructured metal. The free electrons of the metal are able to interact with incident light and generate a localised surface plasmon resonance (LSPR).[19] LSPR can be described as the collective excitation of free electrons around a fixed positive ion centre. This results in an increased absorption of light at the resonance frequency of the oscillation and is reported to be highly dependent on the size, morphology, distribution and the local environment of the nanoparticles.[19,20] To date metals such as Ag and Au have been extensively studied with regards to the LSPR effect due to the fact that the LSPR is found in the visible part of the solar spectrum. This enhanced interaction with light has been reported to increase the absorption cross-section of the catalyst into the visible region and increase its overall activity.[20–23] Other non-reactive metals such as Pd can also produce a plasmon but, as is the case of Pd, have been less extensively studied as the LSPR is centred in the UV part of the spectrum and as such has less technological interest. For example studies by Xiong *et al* have[24] shown that the LSPR for Pd nanocubes of 10nm is limited to wavelengths below 300 nm.

However, there is growing evidence that the LSPR for Pd can be influenced not only the size of the Pd particles but also the local environment of the particles. In 2003 it was demonstrated that there is a strong influence of LSPR position for Pd and refractive index of the substrate and that the LSPR position could red shift by up to 100 nm.[25] The most compelling evidence that the LSPR for Pd can move into the visible part of the spectrum comes from work by Leong *et al*, who have shown that the LSPR for Pd nanoparticles in the size range of 20 – 30 nm was significantly red-shifted from the expected UV position into the visible region at around 500 nm.[26] This work indicates that there may be some significant advantages in using Pd nanostructures in photocatalysts if the size and morphology of the Pd structure can be controlled to increase both light harvesting and effective surface activity. As such there is renewed interest in Pd nanostructures as they

[a] *School of Engineering and Materials Science, Queen Mary, University of London, Mile End Road, E14NS,London, UK*
[b] *School of Chemistry, University of Manchester, Oxford Road, M13 9NJ, Manchester, UK*
Electronic Supplementary Information (ESI) available: [details of any supplementary information available should be included here]. See DOI: 10.1039/x0xx00000x

afford an interesting new approach to visible light photocatalysis as the interaction with light can be driven towards the visible portion of the spectrum as Pd shows excellent catalytic activity compared with Ag and Au.[27,28]

Here we report the reactivity of a photocatalyst composed of Pd nanoparticles on TiO_2 ($Pd:TiO_2$). Our tests follow the decolourisation of rhodamine b dye (RhB) under solar, UV and full visible light irradiation giving a $t_{1/2}$ value of 0.5 minutes. This represents a 19-fold increase in activity compared with untreated, and a significant improvement over the previously published literature data which gives $t_{1/2}$ values at around 7 minutes under solar and visible light irradiation.[29,30]

Experimental

The $Pd:TiO_2$ catalyst was prepared via the photochemical reduction of Pd metal from a $PdCl_2$ solution onto commercially available TiO_2 (Evonik P25) under UV irradiation (see SI for details). The BET (Brunauer-Emmet-Teller) surface area was measured at 52 m^2/g and the Pd loading was determined via ICP (inductively coupled plasma) to be 0.5 wt %. The deposited nanoparticles were confirmed to be metallic Pd by XPS and ranging in size from 1.8 nm to 3.0 nm as determined through TEM analysis. The distribution of the Pd nanoparticles and the morphology of the catalyst are shown in **Figure 1**.

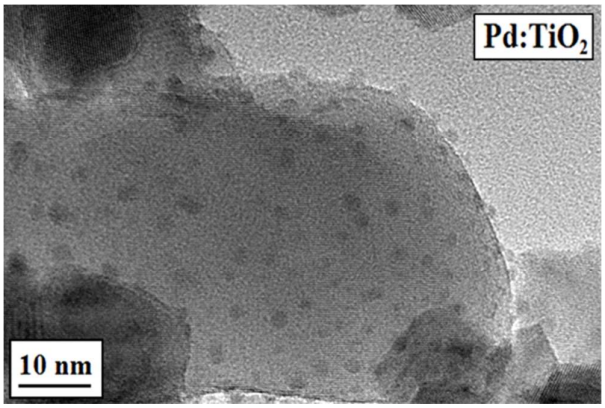

Figure 1 TEM micrograph of the $Pd:TiO_2$ photocatalyst showing Pd nanoparticles as hemispherical artefacts distributed on the TiO_2 support. The Pd is well dispersed in a range of sizes to a maximum of 3 nm

The Pd nanoparticles are well dispersed on the P25 although the distribution appears to be uneven across the surface. XRD data from the particles indicated that there was no change to the TiO_2 crystal structure and that the loading of Pd was too low to be detected by the diffractometer. Diffuse reflectance (DR) analysis measured an increase in light absorption in the visible region for the Pd:TiO2 compared with that of P25 as shown in **Figure 2**.

An increase to 8% increase in light harvesting capability of the catalyst was calculated from the normalized spectra, which highlighted the change in the absorption profile of the new catalyst and where no anamorphic effects were observed after normalization.

The onset of absorption for P25 is in agreement with that of the literature (~ 390 nm) and the band gap was estimated to be 3.23 eV as is expected for a TiO_2 substrate. However, Figure 2 clearly shows a new feature in the absorption spectra for the $Pd:TiO_2$ system that must be explained in order to fully understand the improvement of photocatalytic performance for this new system. The $Pd:TiO_2$ exhibits a broad absorption into the visible region with the peak centred at 456 nm and an estimated energy band gap of 3.19 eV. The band gap is within error for the measurements undertaken and so is associated with the direct band to band transition in the TiO_2. The peak centred around 456 nm is believed to be a characteristic of a local surface LSPR for the Pd nanoparticles.

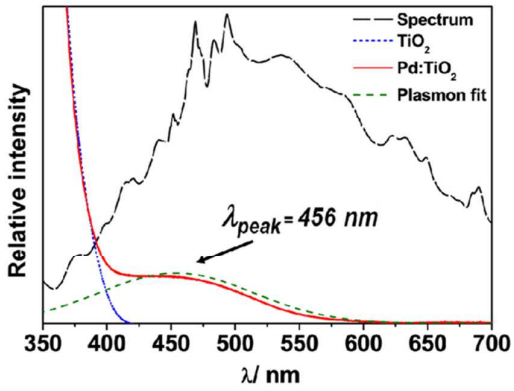

Figure 2 Normalized absorption specrtra of DR measurements of $Pd:TiO_2$ compared with P25

That nanostructured Pd can develop a LSPR is not in question as there are various contributions to the literature indicating both theoretical and practical examples of a plasmonic interaction.[24,31] Indeed, similar metal systems such as Au and Ag have very well documented LSPR. The location of the LSPR peak in our system is significantly red-shifted over that for the theoretical position of the Pd system when considered in a vacuum. However, there is evidence of a red shift in the LSPR peak when Pd nanostructures are developed on the surface of dielectric material such as in our system. These red shifts can be up to 100 nm so if we have the theoretical position of the LSPR centred around 300 nm and red shift by 100 nm the centre for the LSPR in this supported system could reside around 400 nm. Our measured LSPR centre point is 456 nm which is now on the order of that expected. One additional piece of evidence to support our assertion that the Pd nanoparticles are producing a LSPR at *ca* 450 nm comes from recent work where a Pd LSPR was described at more than 550 nm. In that case the Pd nanoparticles were around 20 to 30 nm in cross section compared to our 3 – 5 nm particle size. A study by Langhammer et al. showed that reducing the Pd particle size blue shifts the LSPR centre point.[31] It therefore seems more than reasonable that our Pd nanoparticles are generating a LSPR at *ca* 450 nm due to the size of the particles and interaction with the supporting media as has been predicted by theory.

In order to determine whether the increased light harvesting potential of Pd:TiO_2 would directly translated to an increase in the photocatalytic efficiency of the system. This was done by testing the efficiency of the catalyst in the photodecolourisation of RhB under simulated sunlight and using optical filters to block regions of the spectrum and determine the activity of the catalyst under these conditions. The irradiance value from the solar simulator was adjusted when using the optical filters to compensate for the reduction in transmittance. When a filter was used the power of the solar simulator was adjusted to match the irradiance value to the same value as when no filter was used. This ensured that there was no loss of irradiation intensity at the incoming regions.

The decolorization of RhB in the presence of Pd:TiO_2 was monitored by measuring the change in the absorbance value of the dye over time at λ_{max} = 554 nm following the Beer-Lambert law. This process was carried out over 6 experiments using optical filters to block irradiation at λ > 400 nm (VIS block) and also at λ < 400 nm (UV block) where P25 was used as a reference. In order to fully determine the impact of the presence of the photocatalysts a control experiment was also carried out in the absence of photocatalyst, see SI for results of control test. The catalysts and optical filters used, as well as the calculated $t_{1/2}$ and rate of reaction values of RhB are given in **Table 1**.

Table 1 The photocatalytic activity of Pd:TiO_2 compared with P25.

Photocatalyst	Filter used	$t_{1/2}$/ minutes	k_{app}/ $minute^{-1}$
P25	No filter	9.4	0.073
	VIS block	19.3	0.04
	UV block	63.6	0.011
Pd:TiO_2	No filter	0.5	1.410
	VIS block	3.1	0.226
	UV block	8.5	0.078

The decolourisation pathway and mechanism for the degradation of RhB has been reported elsewhere[32–34] for TiO_2 based catalysts and it is thought that the degradation of RhB in the presence of the Pd:TiO_2 co-catalyst undergoes a similar pathway.

The fastest $t_{1/2}$ value was measured for the Pd:TiO_2 catalyst under full solar irradiation. This value constitutes a 19-fold increase in activity compared with TiO_2 under identical conditions. Under visible irradiation with the UV blocked the reaction rate of P25 was the lowest value of any catalyst tested. The reduced activity observed under these conditions is attributed to the photo-assisted oxidation (PAO) of the dye, which has been previously well reported.

Under full solar irradiation our Pd:TiO_2 gave the fastest $t_{1/2}$ value. Employing a filter that only let the UV portion of the spectrum pass (λ < 400 nm) the reaction rate of P25 was reduced compared when compared to the activity under full solar irradiation. When illuminated with the same portion of the solar spectrum the Pd:TiO_2 catalyst also showed a reduced reaction rate that was intermediate when compared to its activity under full spectrum and visible spectrum irradiation. The decolourization rate profiles for P25 and Pd:TiO_2 in the RhB decolorization experiments are shown in **Figure 3** (A comparison of the catalytic performance of this catalyst compared with other Pd-TiO_2 systems can be found in the SI).

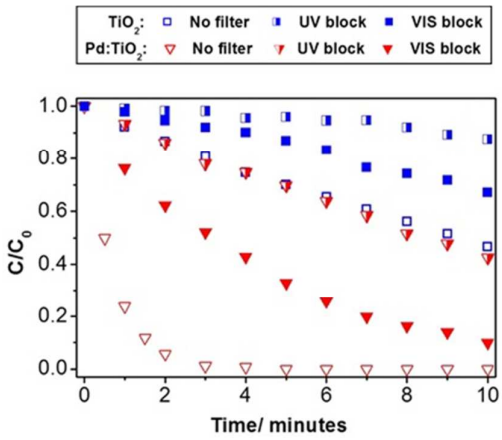

Figure 3 Normalized RhB decolourisation curves in the for P25 and Pd:TiO_2 photocatalysts under different regions of the spectrum

As can be seen from Figure 3 the Pd:TiO_2 catalyst outperforms unmodified P25 in all the experimental conditions. Further review of Figure 3 shows that there is a requirement for a contribution from the UV and visible portion of the spectrum for the Pd:TiO_2 catalyst to perform at the optimum rate.

The presence of the Pd nanoparticles was found to enhance the optical response of the photocatalyst up to ~ 600 nm, which constitutes an increase of 8% compared with P25. This altered absorption profile improved the photocatalytic activity of Pd:TiO_2 and this can be explained by the LSPR effect of the Pd nanoparticles as depicted in **Figure 4**.

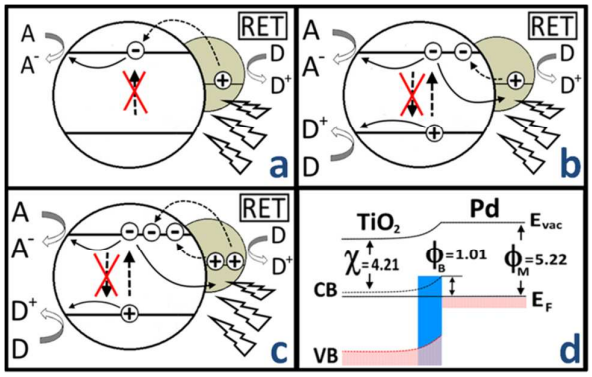

Figure 4 Schematic representation of the mechanisms thought to be occurring during photocatalyst excitation by different regions of the spectrum where a) shows that excited electrons can overcome the Schottky barrier and transfer to the TiO_2 via resonant energy transfer (RET) from the Pd, promoting oxidation on the Pd under

visible light irradiation b) Under UV irradiation, charge carriers are generated within TiO_2. The LSPR of Pd also extends into the UV region where RET can occur leading to charge transfer to TiO_2 and oxidation on Pd c) the combination of these processes results in the enhanced photocatalytic activity of the system d) shows the Schottky barrier formed at the metal/ semiconductor interface and the values of χ, ϕ_B and ϕ_M, which are the TiO_2 electron affinity, barrier height and the Pd work function, respectively.

In order to explain the need for full spectrum illumination it seems reasonable that two processes are taking place on the catalyst. One mechanism attributed to the LSPR where electrons in the Pd are excited sufficiently to overcome the Schottky barrier at the semiconductor/ metal interface and transfer 'hot electrons' to the TiO_2 (Figure 4a) has been previously reported.[35] The height of the Schottky barrier (ϕ_B) formed at the Pd/TiO_2 junction was calculated at 1.10 eV (Figure 4d and details in SI), making it possible for visible irradiation to excite electrons into the conduction band of TiO_2. 'Hot holes' remaining in the metal nanoparticle can react with adsorbed species and further increasing the reactivity of the co-catalyst.[36]

The other mechanism occurs under super band gap irradiation where electron excitation within the TiO_2 occurs (Figure 4b). Hot electrons are also excited from the Pd nanoparticle to the conduction band of TiO_2. The activity of the catalyst is therefore, further increased by a combination of these processes. If, as has been reported, there is the additional contribution that charge recombination is suppressed due to the Pd nanoparticles on the surface of the TiO_2 there is an increase in carrier lifetimes which will still further enhance the performance of the catalyst.

We believe that the trapping of electrons in our system is particularly effective as a result of the hemispherical morphology of the supported Pd (Figure 1). This morphology is the result of the nucleation and growth of Pd nanoclusters on electron rich defect sites in the P25 lattice. The defect sites promote the photochemical reduction of Pd at preferential locations from where the deposited nanoparticles can then grow and form the hemispherical nanostructures. This process is markedly different form the precipitation of spherical nanoparticles formed in solution onto a substrate. Compared with systems in which hemispherical metal nanoparticles are present on the surface of a semiconductor, there is a larger contact area between the metal and the semiconductor for the hemispherical structures. This provides a larger pathway for the transfer and trapping of photo-excited electrons to the Pd thus, improving charge separation and increasing the charge carrier lifetimes.

In comparison with similar metal-TiO_2 systems, we found that the combination of the LSPR and the improved charge carrier trapping of the Pd nanoparticles under full solar irradiation results in a beneficial synergistic effect that gives a high photodecolourisation rate of RhB dye.

Our experiments also show that in order for both mechanisms discussed above to occur simultaneously, there is a need for full solar irradiation (Figure 4c) which results in the highest rate of reaction.

Conclusions

By developing a nanostructured Pd:TiO_2 catalyst we have developed a system that demonstrates a LSPR for a Pd nanoparticle in the visible part of the spectrum. Our LSPR centred around *450* nm is significantly red shifted when compared to the theoretical position of the LSPR but fits the trends seen with the most recent work published on the topic of a Pd LSPR, and interaction with the TiO_2 support. The combination of a highly catalytic metal nanostructure capable of interaction with a photocatalyst leads to 19-fold increase in the decolourisation rate of a typical commercial dye material under full solar irradiation. Our evidence for the LSPR effect comes from selective filtering of the incident light used in photocatalyst experiments, analysis of the diffuse reflectance spectrum and review of the available literature in the area.

Notes and references

‡ Footnotes relating to the main text should appear here. These might include comments relevant to but not central to the matter under discussion, limited experimental and spectral data, and crystallographic data.

(1) Chong, M. N.; Jin, B.; Chow, C. W. K.; Saint, C. *Water Res.* **2010**, *44*, 2997–3027.

(2) Prairie, M. R.; Evans, L. R.; Stange, B. M.; Martinez, S. L. *Environ. Sci. Technol.* **1993**, *27*, 1776–1782.

(3) Hoffmann, M. R.; Martin, S. T.; Choi, W.; Bahnemann, D. W. *Chem. Rev.* **1995**, *95*, 69–96.

(4) Chen, X.; Mao, S. S. *Chem. Rev.* **2007**, *107*, 2891–2959.

(5) Kumar, S. G.; Devi, L. G. *J. Phys. Chem. A* **2011**, *115*, 13211–13241.

(6) Linsebigler, A. L.; Lu, G.; Yates, J. T. *Chem. Rev.* **1995**, *95*, 735–758.

(7) Roy, S.; Varghese, O.; Paulose, M.; Grimes, C. *ACS Nano* **2010**, *4*, 1259–1278.

(8) O'Regan, B.; Grätzel, M. *Nature* **1991**, *353*, 737–740.

(9) Wang, C.-M.; Gerischer, H.; Heller, A. *J. Am. Chem. Soc.* **1992**, *114*, 5230–5234.

(10) Zhao, J.; Wu, T.; Wu, K.; Oikawa, K. *Environ. Sci. Technol.* **1998**, *32*, 2394–2400.

(11) Wu, T.; Liu, G.; Zhao, J.; Serpone, N. *J. Phys. Chem. B* **1998**, *5647*, 5845–5851.

(12) Aarthi, T.; Madras, G. *Ind. Eng. Chem. Res.* **2007**, 7–14.

(13) Liu, Z.; Hou, W.; Pavaskar, P.; Aykol, M.; Cronin, S. B. *Nano Lett.* **2011**, *11*, 1111–1116.

(14) Kuvarega, A. T.; Krause, R. W. M.; Mamba, B. B. *J. Phys. Chem. C* **2011**, *115*, 22110–22120.

(15) Zhang, N.; Liu, S.; Fu, X.; Xu, Y. *J. Phys. Chem. C* **2011**, *2*, 9136–9145.

(16) Liu, R.; Wang, P.; Wang, X.; Yu, H.; Yu, J. *J. Phys. Chem. C* **2012**, *116*, 17721–17728.

(17) Cui, Y.; Briscoe, J.; Dunn, S. *Chem. Mater.* **2013**, *25*, 4215–4223.

(18) Stock, M.; Dunn, S. *IEEE Trans. Ultrason. Ferroelectr. Freq. Control* **2011**, *58*, 1988–1993.

(19) Hutter, E.; Fendler, J. H. *Adv. Mater.* **2004**, *16*, 1685–1706.

(20) Noguez, C. *J. Phys. Chem. C* **2007**, *111*, 3806–3819.

(21) Lu, X.; Rycenga, M.; Skrabalak, S. E.; Wiley, B.; Xia, Y. *Annu. Rev. Phys. Chem.* **2009**, *60*, 167–192.

(22) Kochuveedu, S.; Kim, D. D. *J. Phys. Chem. C* **2012**, *116*, 2500–2506.

(23) Cushing, S. K.; Li, J.; Meng, F.; Senty, T. R.; Suri, S.; Zhi, M.; Li, M.; Bristow, A. D.; Wu, N. *J. Am. Chem. Soc.* **2012**, *134*, 15033–15041.

(24) Xiong, Y.; Chen, J.; Wiley, B.; Xia, Y.; Yin, Y.; Li, Z. Y. *Nano Lett.* **2005**, *5*, 1237–1242.

(25) Kelly, K. L.; Coronado, E.; Zhao, L. L.; Schatz, G. C. *J. Phys. Chem. B* **2003**, *107*, 668–677.

(26) Leong, K. H.; Chu, H. Y.; Ibrahim, S.; Saravanan, P. *Beilstein J. Nanotechnol.* **2015**, *6*, 428–437.

(27) Campelo, J. M.; Luna, D.; Luque, R.; Marinas, J. M.; Romero, A. a. *ChemSusChem* **2009**, *2*, 18–45.

(28) Nørskov, J. K.; Ressmeisl, J.; Logadottir, a.; Lindqvist, L.; Kitchin, J. R.; Bligaard, T.; Jonsson, H. *J. Phys. Chem. B* **2004**, *108*, 17886–17892.

(29) Zhang, Q.; Lima, D. Q.; Lee, I.; Zaera, F.; Chi, M.; Yin, Y. *Angew. Chemie - Int. Ed.* **2011**, *50*, 7088–7092.

(30) Yu, K.; Yang, S.; He, H.; Sun, C.; Gu, C.; Ju, Y. *J. Phys. Chem. A* **2009**, *113*, 10024–10032.

(31) Langhammer, C.; Yuan, Z.; Zorić, I.; Kasemo, B. *Nano Lett.* **2006**, *6*, 833–838.

(32) Cui, Y.; Goldup, S. M.; Dunn, S. *RSC Adv.* **2015**, *5*, 30372–30379.

(33) Li, J.; Ma, W.; Chen, C.; Zhao, J.; Zhu, H.; Gao, X. *J. Mol. Catal. A Chem.* **2007**, *261*, 131–138.

(34) LI, J.; MA, W.; LEI, P.; ZHAO, J. *J. Environ. Sci.* **2007**, *19*, 892–896.

(35) Sá, J.; Tagliabue, G.; Friedli, P.; Szlachetko, J.; Rittmann-Frank, M. H.; Santomauro, F. G.; Milne, C. J.; Sigg, H. *Energy Environ. Sci.* **2013**, *6*, 3584–3588.

(36) Clavero, C. *Nat. Photonics* **2014**, *8*, 95–103.